Observation of Vortex Coalescence in the Anisotropic Spin-Triplet Superconductor Sr_2RuO_4

V. O. Dolocan,[1] C. Veauvy,[1] F. Servant,[1] P. Lejay,[1] K. Hasselbach,[1] Y. Liu,[2] and D. Mailly[3]

[1]*CRTBT-CNRS, 25 Avenue des Martyrs, 38042 Grenoble, France*
[2]*The Pennsylvania State University, University Park, Pennsylvania 16802, USA*
[3]*LPN-CNRS, Route de Nozay, 91460 Marcoussis, France*

We present direct imaging of magnetic flux structures over the *ab* face of the anisotropic, spin-triplet superconductor Sr_2RuO_4 using a scanning μSQUID force microscope. Individual vortices with a single flux quantum were observed at low magnetic fields applied along the out-of-pane direction. At intermediate fields, the direct imaging revealed coalescing of vortices and the formation of flux domains. Our observations imply the existence of a mechanism in this material for bringing vortices together overcoming the conventional repulsive vortex-vortex interaction.

Sr_2RuO_4 is a tetragonal, layered perovskite superconductor with a superconducting transition temperature (T_c) of 1.5 K [1]. Sr_2RuO_4 has been a subject of intensive interest in recent years because of the theoretical suggestion [2,3] that Sr_2RuO_4 is an odd-parity, spin-triplet superconductor. Abundant experimental evidence supporting the theoretical prediction has been obtained, as summarized recently [4,5]. A very recent phase-sensitive experiment [6] has established the odd-parity pairing symmetry in Sr_2RuO_4 by measuring the quantum interference pattern in superconducting quantum interference devices (SQUIDs) consisting of Sr_2RuO_4 and $Au_{0.5}In_{0.5}$, an *s*-wave superconductor. In addition, muon spin rotation (μSR) experiments have revealed [7] the presence of spontaneous currents in the superconducting Sr_2RuO_4, indicating the breaking of time reversal symmetry (TRS) below T_c. The TRS breaking implies that the Cooper pair has an internal orbital moment (chirality) giving rise to a superconducting order parameter with multiple components.

The crystal structure and the thermodynamic properties of the superconductor restrain the choice of the order parameter. The orbital component of the order parameter of the form, $(p_x \pm ip_y)$ is compatible with most experiments. The two possible realizations of the superconducting order parameter, $p_x + ip_y$ ($p+$) and $p_x - ip_y$ ($p-$), represent two possible chiral states [8] which are energetically degenerate. Consequently the presence of domains in which the Cooper pairs possess different orbital angular momentum is expected. Building on this form of the order parameter, the magnetization processes were explored by numerical simulations [9,10]. In a magnetic field the degeneracy between $p+$ and $p-$ domains is lifted, favoring a domain with the Cooper pair orbital moment aligned with the field. The favored domains will have a higher critical field H_{c2}, and a lower H_{c1}. Consequently, vortices will first appear in these domains. At the interface between the domains of opposite chiralities, walls will form [11]. The presence of domain walls has considerable influence on the

vortex motion and pinning. For example, flux penetration should take place preferentially along the domain walls. These walls will act as preferential pinning sites for vortices. Vortices at these sites could decompose into fractional vortices decorating the domain walls. In analogy with the case of superfluid ^{3}He-*A* decorated domain walls are called vortex sheets [12,13].

Thus the visualization of vortices is an important step for elucidating the unconventional superconductivity in Sr_2RuO_4. μSR [14] and small angle neutron scattering [15] (SANS) measurements revealed formation of a square vortex lattice in Sr_2RuO_4 when the magnetic field was applied along the *c* axis and for fields ranging between 50 and 300 G (field cooling). The square lattice and the detail of the magnetic field distribution around the vortices were found to agree qualitatively with a two-component *p*-wave Ginzburg-Landau theory [16–18]. However, SANS is a bulk probe that is sensitive to the long-range correlation in the vortex state rather than to the local structure. Scanning tunneling microscopy on Sr_2RuO_4 did not succeed to image vortices. The reason may lay with the observed reconstruction [19,20] of the surface of Sr_2RuO_4, suppressing superconductivity at an atomic length scale.

Here we present the first microscopic images of the magnetic flux state in Sr_2RuO_4, using a custom-built μSQUID force microscope (μSFM) [21,22]. The μSFM is a sensitive tool for observing individual vortices on a local scale with a spatial resolution of 1 μm. The μSQUID loop is scanned parallel above the surface of the sample. The component of the local magnetic field perpendicular to the surface induces critical current variations in the μSQUID. These variations are recorded as the detector scans the surface of the sample. The distance between the sample and the μSQUID is kept constant during scanning, as the mechanical force between the μSQUID tip and the sample is regulated. The distance between μSQUID and sample depends on the approach angle and the position of the μSQUID loop relative to the tip. The microscope is placed

at the center of two copper coils at room temperature, a solenoid and rotatable Helmholtz coil, which allow us to apply magnetic field in any direction of space.

The Sr_2RuO_4 single crystal was grown by a floating zone technique using an image furnace [23]. Specific heat measurements of crystals taken from the same single-crystal rod showed volume superconductivity below a temperature of 1.31 K and a transition width of less than 0.1 K. We used 2 different samples of platelike shape of this crystal, one having a thickness of 0.5 mm with an estimated demagnetization factor, N, of 0.9 (sample 1) and the other 0.6 mm with $N = 0.7$ (sample 2).

During the imaging, the μSQUID moved in a plane above a cleaved ab surface of the single crystal of Sr_2RuO_4. Round shaped flux structures are seen after cooling the crystal (sample 1) in a magnetic field of 0.1 G applied along the c axis (Fig. 1). The measured field profile at locations 2, 3, and 4 can be well adjusted to the model [24] of a single quantized vortex using values for the SQUID-sample distance between 1.2 ± 0.1 μm and a penetration depth $\lambda_{ab} = 0.15$–0.2 μm. The fit and the experimental flux profile of vortex 2 are presented in Fig. 1(b). We fit the experimental data using the penetration depth λ_{ab} and the height of the SQUID loop above the ab plane as parameters. The value for λ_{ab} is in agreement with the literature values, and the SQUID-sample distance is consistent with the setup. A vortex in the sample induced a flux variation of 0.07 Φ_0 in the μSQUID. Single vortices are present at locations 2, 3, and 4, and a vortex pair at location 1 (two unresolved vortices close together). The vortex at location 4 is close to a crystal defect. The observed flux structures were seen to disappear completely above $T = T_c = (1.35 \pm 0.05)$ K, in agreement with the T_c value determined previously in specific heat measurements. At these low fields Sr_2RuO_4 behaves as a usual type-II superconductor.

The images of Fig. 2 were obtained after field cooling (FC) sample 2 in fields between 2 and 7 G to a temperature of 0.35 K. At 2 G applied field, Fig. 2(a), vortices are distinct, some of them are close together, at 6 G Fig. 2(b) a higher density of individual vortices is detected, locally coalescing flux regions form, and as the field increases
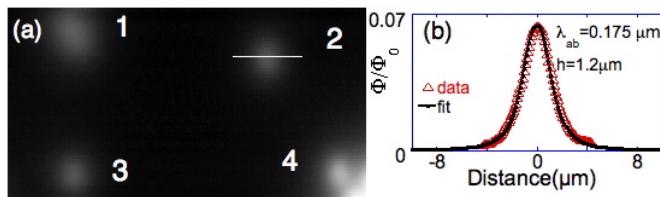
further to 7 G, Fig. 2(c) the individual vortices have melted into flux domains. For comparison, we imaged a conventional s-wave superconductor $NbSe_2$ having a T_c of 7.2 K. $NbSe_2$ is a layered material; it is weakly anisotropic with an effective mass anisotropy (λ_c/λ_{ab}) of 3.3. The penetration depth for applied fields along c axis λ_{ab} is 0.15 μm comparable with λ_{ab} of Sr_2RuO_4. A hexagonal vortex lattice is readily observed by the μSFM Fig. 2(d), after field cooling the sample in 5 G. The vortices are clearly distinct from one another. When the field is further increased the vortices in $NbSe_2$ approach so close that μSFM cannot resolve the vortices anymore and the flux appears homogenous. The case of Sr_2RuO_4 is different: instead of the formation of a vortex lattice we observe vortex coalescence. The threshold value of the applied field at which the vortices coalesce depends on the thickness of the sample. A complete collapse of the vortices into one single domain is not observed, probably due to the presence of weak barriers in the material.

Domain walls delimiting regions with angular momentum $l_z = \pm 1$ ($\hat{l}$ is parallel to the c axis) could provide the scenario for weak intrinsic pinning at low magnetic fields. The difference of free energy under magnetic field between the two states may make those vortices appear preferentially in domains of one type. This is in qualitative agreement with our observations of flux-filled and flux-free regions, the flux-filled regions in Figs. 2(b) and 2(c) occupying 60% to 70% of the total area.

There should be a difference between field cooled (FC) and zero-field cooled (ZFC) experiments. Under ZFC conditions, domains of each chirality should be equally present. Upon subsequent field increase the vortex should penetrate by the domain walls and then enter from the edge preferentially in the p-wave domain. We made ZFC experiments and increased the applied field subsequently. At
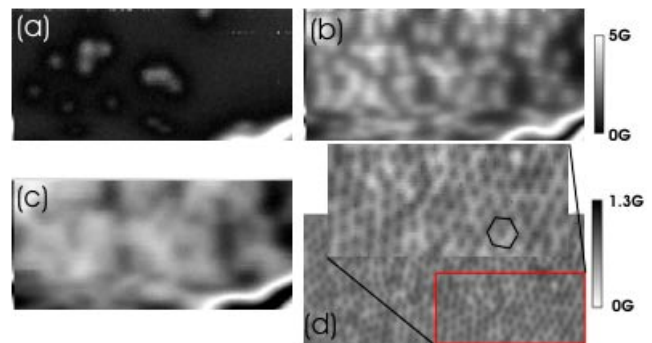

FIG. 1 (color online).   (a) A μSFM image of the ab face of Sr_2RuO_4, at $T = 0.36$ K, $H = 0.1$ G ($H\|c$, FC at 0.1 G). The imaged area is 31×17 μm^2. (b) A flux profile of the vortex at the location 2 and a fit are shown in fractions of Φ_0 of the μSQUID. At location 1 the flux is due to two vortices close by. Single vortices are situated at locations 2, 3, and 4. At location 4 the vortex is in proximity to a defect.

FIG. 2 (color online). Comparison between $NbSe_2$ and Sr_2RuO_4 for magnetic fields applied perpendicular to the ab plane. (a) A μSFM image after field cooling Sr_2RuO_4 in a field of 2 G, (b) in 6 G, and (c) in 7 G. The imaging temperature is 0.35 K for all images. Coalescence of vortices is observed. (d) A μSFM image of a vortex lattice in $NbSe_2$. The data are acquired after field cooling the $NbSe_2$ crystal in 5 G at a temperature of 1.1 K. The inset shows the hexagonal order of the lattice. For all images the imaging area is 62 μm $\times$ 30 μm.

fields less than H_{c1} we observe only a few single vortices, the shielding currents at the surface retain the vortices, while above H_{c1}, at about 30 G, vortices penetrate massively into the center of the sample. The observed flux profile is not flat but it is modulated, confirming the observation that vortices coalesce.

How strongly are these domains attached to the crystal? In order to examine the stability of the domain configuration the in-plane field was raised while the c axis field was kept constant and then the microscope imaged the same area again. Figure 3 shows for increasing in-plane fields how the condensed vortex structures rearrange freely in order to accommodate the experimental conditions: for 0 G in-plane field and 2 G FC applied parallel with c axis in the sample 1 we see only domains of flux, Fig. 3(a). The difference in flux density between the bright (vortex) and the dark (vortex-free) regions is 3.5 G. Integration of the flux pattern gives an average field of 1.4 ± 0.2 G at the μSQUID, close to the applied field of 2 G, the vortices are condensed in domains, leaving empty of flux entire regions of the superconductor.

At 5 G in-plane applied field, the flux domains become slimmer and above 10 G the flux domains are seen to evolve into line-shaped structures. The number of flux domains was found to increase in a regular fashion with the in-plane field amplitude. This regular increase of the flux domain density and their temperature evolution (data not shown) suggest that the flux structures are unrelated to any structural defects in the crystal as defect pinning [25] of vortices would interfere with regularly spaced vortex pattern.

The line-shaped flux structures evoke vortex chains observed in decoration experiments of $YBa_2Cu_3O_{7+\delta}$ [26] and $Bi_2Sr_2CaCu_2O_{8+\delta}$ [27]. There, vortex chains appear when the applied field is close to the in-plane direction of the anisotropic superconductor. Sr_2RuO_4 has an effective mass anisotropy 6 times higher than $NbSe_2$ and 4 times higher $YBa_2Cu_3O_{7+\delta}$ but lower than

$Bi_2Sr_2CaCu_2O_{8+\delta}$. Therefore, the arrangement of the domains in lines may be driven by anisotropy.

The attraction between vortices in anisotropic superconductors comes from the misalignment between the vortex axis (B) and the direction of the applied field (H) giving raise to a net transverse magnetization M. This attractive interaction [28] between the vortices is directed along the plane spanned by the anisotropy axis and the in-plane applied field. In agreement with this reasoning we observe that the linear pattern follows the direction of the applied field when the field is rotated in the ab plane (images not shown). The fact that the vortex chains arrange as a function of the field direction and field amplitude shows that the coalescence of the vortices in domains does not originate from defects as the magnetic energies in play can transform these domains into vortex chains.

We followed the evolution from regular straight flux domains to the large domains observed under perpendicular field. Therefore, we monitored the evolution of the flux domain structure while the applied field was tilted away from the in-plane direction, at constant amplitude, increasing in this manner the perpendicular field component. In Fig. 4, the field amplitude, H, was constant at 10 G and the tilting angle was changed. Each data set was acquired after field cooling. In the panel (a) of Fig. 4, a flux domain oriented along the field direction and single vortices are clearly seen; a small defect is present on the bottom right corner. The domain aligns along the direction of the tilted field. As the perpendicular field is increased more magnetic flux enters the sample surface. The flux domains extend and merge with the individual vortices Fig. 4(b) and at higher perpendicular fields we see only domains of flux. The further increase of the perpendicular component increases the density of vortices, thus more domains appear in Fig. 4(c), though the domains are less straight, they start to deform and branch. One reason may be that the vortex density is so high that the vortex-vortex repulsion effective at short distances competes with the attractive interaction
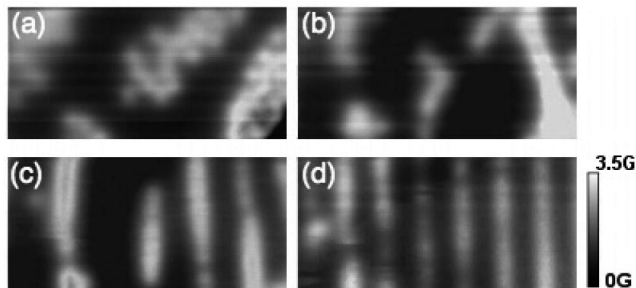

FIG. 3.   SμSFM images of flux domains in Sr_2RuO_4 at $T = 0.36$ K after field cooling at various fields. In all cases, the magnetic field amplitude applied along c axis ($H_\perp$) was kept constant at 2 G while in-plane field (H_{ab}) was (a) 0 G, (b) 5 G, (c) 10 G, (d) 50 G. The imaging area is 31 μm × 17 μm. Field scale in G is shown on the right; dark regions are superconducting vortex-free regions.
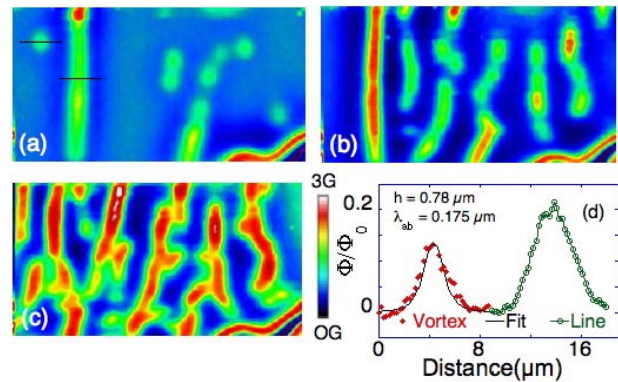

FIG. 4 (color online).   Magnetic images of the flux structures in Sr_2RuO_4 at $T = 0.38$ K with magnetic field H kept constant at 10 G and tilted from c axis with an angle θ (a) 70°, (b) 60°, (c) 50°. The flux density scale is shown on the right of (c). Panel (d) shows a line plot along the line drawn in panel (a).

along the lines. Figure 4(d) shows a line plot along the line drawn in Fig. 4(a). The lines have a width of the order of a vortex. The amplitude of the line is higher as the vortices are dense in the line. We could not explore the question of the possible presence of fractional vortices at the domain walls, as we cannot resolve individual vortices in the domains.

Vortex coalescence overcoming the usual vortex-vortex repulsion is predicted for superconductors with the Ginzburg-Landau parameter $\kappa = \lambda/\xi$ close to $1/\sqrt{2}$ [29]. Sr_2RuO_4 has a λ/ξ value ~ 2 when the magnetic field is directed along the c axis. Individual vortices, the signature of type-II superconductivity, are present in the sample at low fields after field cooling, but no domains are observed, clearly designating Sr_2RuO_4 as a type-II superconductor.

A delicate interplay between anisotropy and unconventional superconductivity may be at the origin of the vortex arrangements we observe. At low perpendicular fields flux domains form, tilting the field, anisotropy effects become important so the vortices try to align along the field direction. As the normal field component increases the vortex density increases and the vortex-vortex repulsion starts to destroy the linear vortex chain structure. At high flux density the vortices come so close that the vortex-vortex repulsion generates the square lattice observed in SANS.

Thus the unconventional nature of the superconducting state in Sr_2RuO_4 plays a role in the observed phenomena. The systematic variation of the vortex patterns with the amplitude and orientation of the applied field suggests that they are related to intrinsic physical processes in the superconducting state of this material. Therefore, the formation of the domains may be due to the presence of a chiral superconducting order parameter leading to the formation of the domains and domain walls. More theoretical and experimental work is needed to clarify the physical origins of the observed vortex coalescence and issues raised in the present work.

[1] Y. Maeno *et al.*, Nature (London) **372**, 532 (1994).

[2] T. M. Rice and M. Sigrist, J. Phys. Condens. Matter **7**, L643 (1995).

[3] G. Baskaran, Physica B (Amsterdam) **223**, 490 (1996).

[4] A. P. Mackenzie and Y. Maeno, Rev. Mod. Phys. **75**, 657 (2003).

[5] Y. Maeno, T. M. Rice, and M. Sigrist, Phys. Today **54**, No. 1, 42 (2001).

[6] K. D. Nelson, Z. Q. Mao, Y. Maeno, and Y. Liu, Science **306**, 1151 (2004).

[7] G. M. Luke *et al.*, Nature (London) **394**, 558 (1998).

[8] V. P. Mineev and K. V. Samokhin, *Introduction to Unconventional Superconductivity* (Gordon and Breach, New York, 1998).

[9] M. Ichioka and K. Machida, Phys. Rev. B **65**, 224517 (2002).

[10] M. Ichioka, Y. Matsunaga, and K. Machida, Phys. Rev. B **71**, 172510 (2005).

[11] M. Sigrist and D. F. Agterberg, Prog. Theor. Phys. **102**, 965 (1999).

[12] Y. Matsunaga, M. Ichioka, and K. Machida, Phys. Rev. Lett. **92**, 157001 (2004).

[13] U. Parts *et al.*, Phys. Rev. Lett. **72**, 3839 (1994).

[14] C. M. Aegerter *et al.*, J. Phys. Condens. Matter **10**, 7445 (1998).

[15] P. G. Kealey *et al.*, Phys. Rev. Lett. **84**, 6094 (2000).

[16] D. F. Agterberg, Phys. Rev. B **58**, 14484 (1998).

[17] R. Heeb and D. F. Agterberg, Phys. Rev. B **59**, 7076 (1999).

[18] T. Kita, Phys. Rev. Lett. **83**, 1846 (1999).

[19] R. Matzdorf *et al.*, Science **289**, 746 (2000).

[20] A. Damascelli *et al.*, Phys. Rev. Lett. **85**, 5194 (2000).

[21] C. Veauvy, D. Mailly, and K. Hasselbach, Rev. Sci. Instrum. **73**, 3825 (2002).

[22] C. Veauvy, K. Hasselbach, and D. Mailly, Phys. Rev. B **70**, 214513 (2004).

[23] F. Servant, Ph.D. thesis, Universite Joseph Fourier, 2002.

[24] J. R. Kirtley, V. G. Kogan, J. R. Clem, and K. A. Moler, Phys. Rev. B **59**, 4343 (1999).

[25] D. A. Huse, Phys. Rev. B **46**, 8621 (1992).

[26] P. L. Gammel, D. J. Bishop, J. P. Rice, and D. M. Ginsberg, Phys. Rev. Lett. **68**, 3343 (1992).

[27] C. A. Bolle *et al.*, Phys. Rev. Lett. **66**, 112 (1991).

[28] A. I. Buzdin and A. Yu. Simonov, Zh. Eksp. Teor. Fiz. **98**, 2074 (1990) [Sov. Phys. JETP **71**, 1165 (1990)].

[29] F. Mohamed, M. Troyer, G. Blatter, and I. Luk'yanchuk, Phys. Rev. B **65**, 224504 (2002).